

## EXPERIMENTAL RESULTS ON MICROSHIELD TRANSMISSION LINE CIRCUITS

T. M. Weller, G. M. Rebeiz, and L. P. Katehi

*NASA Center for Space Terahertz Technology  
The University of Michigan  
Ann Arbor MI 48109-2122*

**Abstract** — Presented here are the first experimental data on microshield circuits which use the membrane technology. Microshield shows potential for improved performance relative to current planar transmission line geometries. This paper will describe results on stepped-impedance filters and coplanar waveguide-to-microshield transitions.

### I. INTRODUCTION

This paper presents for the first time an extensive experimental study of microshield transmission line circuits which are fabricated using membrane technology [1]. The microshield line was introduced in 1991 and has been shown, using proven theoretical techniques, to exhibit desirable waveguiding properties [2]. These properties include pure TEM propagation and zero dispersion in a wide, single mode frequency band, low radiation loss, zero dielectric loss, and a broad range of possible line impedance. The lower shielding cavity, furthermore, provides ground plane equalization and thus eliminates the need for air bridges or via holes.

Several types of microshield circuits have now been fabricated and measured, including filters, stubs, and transitions from grounded coplanar waveguide (gcpw) to microshield. The transitions are of immediate interest because the preferred measurement technique requires initial contact to gcpw, as discussed below. Additionally, transmission lines with drastic step changes in the dielectric material may provide novel capabilities and are worthy of investigation. Stepped-impedance filters are examined since they are simple to design and are shown to effectively demonstrate microshield performance. The fabrication and characterization of the transitions and filters are reviewed here.

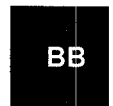
### II. FABRICATION AND DESIGN

The foremost characteristic of microshield circuit fabrication is the utilization of the membrane technology described by Rebeiz, et al [1]. For the work described here, 340  $\mu\text{m}$  thick  $<100>$  silicon wafers, with 1.5  $\mu\text{m}$   $\text{SiO}_2/\text{Si}_3\text{N}_4/\text{SiO}_2$  membrane layers, have been used. The mi-

croshield structure is created by first removing photolithographically defined regions from the membrane layer on the back side of the wafer. This pattern serves as an etch mask, allowing pyramidal cavities to be opened in the wafer using anisotropic Si etchants, such as ethylene diamine Pyrocatechol (EDP). The upper membrane layer will behave as an etch stop, thereby forming the exposed membrane surface with a surrounding cavity below [3].

The final steps in the fabrication process are the metallization of the circuit pattern and the cavity sidewalls. A tri-layer photoresist/aluminum/photoresist technique with metal evaporation is used to deposit the circuit pattern on the top side of the membrane layer. Evaporation is also used for metal deposition on the cavity sidewalls, but here some shadowing is required to protect selected areas of the membrane from backside metallization. A diced or micro-machined silicon mask is used to shield the region between the inner-edges of the upper ground planes, thus preventing metallization in the slots. The finished circuits are then mounted on a ground plane to fully enclose the lower shielding cavity. A photograph of a 5- and a 7-section lowpass filter is shown in Figure 1.

An important design objective in this project is to develop a low loss transition from grounded coplanar waveguide to microshield. This is necessary because the measurement device is a microwave probe station, and the probe contacts must be formed in gcpw since the membranes cannot reliably withstand multiple probing attempts. While the design of a transition should include consideration of the characteristic impedance, it must also be considered that each of these lines is a mixed coplanar-microstrip guiding structure, for which the relative slot widths, center conductor width, and ground plane separation all determine the mode of propagation. Guidelines for the design of gcpw can be found in [4, 5], while those for the microshield line are found in [3]. Although one transition design was chosen *a priori* for measurement purposes, three other variations were tested and their performance is reviewed in the following section.



### III. EXPERIMENTAL RESULTS

#### A. (Grounded) CPW to Microshield Transitions

The primary motivation for investigating the gcpw-to-microshield transitions lies in optimizing the design for measurement purposes, as discussed above. One can envision, however, alternative reasons for utilizing short segments of cpw along a microshield line (or vice versa): a simple means of fixed phase delay or advance, as the phase velocity will be lower in cpw than in microshield; mechanical support to facilitate mounting hybrid active devices along a microshield line; and obtaining very large impedance ratios for filter purposes are all possibilities. To our knowledge, such planar transmission line circuits with similar metallization, yet drastic dielectric changes, have not previously been explored.

There were four microshield-gcpw-microshield transitions which were measured. The structures consist of a section of grounded cpw of length  $\frac{\lambda_{g,CPW}}{2}$  at 40 GHz, which is positioned in the center of a microshield line. The design is illustrated in Figure 2. In all cases the microshield geometry has a center conductor width,  $s$ , of 350  $\mu\text{m}$  and a slot width,  $w$ , of 35  $\mu\text{m}$ . The characteristic impedance for this line is 75  $\Omega$ . For the four different designs,  $s + 2w$  in the gcpw was also held constant at 420  $\mu\text{m}$ , and center conductor widths of 35, 70, 140, and 280  $\mu\text{m}$  were tested. These geometries result in characteristic impedances of 88, 71, 54, and 36  $\Omega$ , respectively.

The measured  $S_{11}$  for the transitions is given in Figure 3. The best performance, less than -15 dB from 20 to 40 GHz, is obtained with the 70  $\mu\text{m}$  transition, which is also the design with the closest impedance match. This transition also operates with very low radiation loss, as shown in Figure 4. It should be noted, however, that the  $S_{11}$  response is very dissimilar to that expected from ideal transmission line theory, which would predict a gradual rolloff to a perfect match at 40 GHz. These discrepancies may be partially explained by the field-configuration considerations mentioned above, as the microshield line is operating in a strongly cpw-like mode, whereas the grounded cpw line will exhibit more of a hybrid cpw/microstrip characteristic due to the smaller height-to-slot width ratio.

#### B. Stepped-Impedance Low Pass Filters

Stepped-impedance filters are commonly used for applications which do not require a sharp cutoff, such as in the rejection of out of band mixer harmonics. They are a desirable test circuit for the new microshield technology primarily because they are quite easy to design and their performance may be used to qualify impedance calculations, the degree of TEM mode propagation, and the level of conductor and radiation loss.

A schematic diagram of the 5-section filter design is given in Figure 5. The measured performance for 5- and 7-section 0.5 dB ripple Chebyshev designs is shown in Figure 6. Also shown is the theoretical filter response obtained using ideal transmission line theory, with empirically-derived corrections for the effective line extension at impedance steps [6]. The agreement is quite good, and the differences near cutoff can be explained by the peak in the radiation loss, shown in Figure 7. Also, no correction for conductor loss is included in the theoretical data.

### IV. CONCLUSION

Experimental results on microshield stepped-impedance filters and transitions to grounded coplanar waveguide have been presented. The filter response compared very well to ideal transmission line theory when effective line length corrections for impedance steps were employed. The best transition performance demonstrates an  $S_{11}$  below -15 dB from 20 to 40 GHz.

### V. ACKNOWLEDGEMENT

This work has been supported by the Office of Naval Research under contract No. N00014-92-J-1070 and the NASA Center for Space Terahertz Technology. The authors would like to thank Prof. G. Rebeiz's group for their assistance, and particularly Mr. Walid Ali-Ahmad.

### VI. REFERENCES

- [1] G. M. Rebeiz, D. P. Kasilingam, Y. Guo, P. A. Stimson and D. B. Rutledge, "Monolithic Millimeter-Wave Two-Dimensional Horn Imaging Arrays", *IEEE Trans. on Antennas and Propagation*, Vol. 38, pp. 1473-1482, Sept. 1990.
- [2] N. Dib, W. Harokopus, P. Katehi, C. Ling, and G. Rebeiz, "Study of a Novel Planar Transmission Line," *1991 IEEE MTT-S International Microwave Symposium Digest*, Boston, pp. 623-626.
- [3] N. I. Dib, P. B. Katehi, "Impedance Calculation for the Microshield Line," *Microwave and Guided Letters*, Vol. 2, No. 10, Oct. 1992, pp. 406-408.
- [4] G. Ghione and C. Naldi, "Coplanar Waveguides for MMIC Applications: Effect of Upper Shielding, Conductor Backing, Finite-Extent Ground Planes, and Line-to-Line Coupling," *IEEE Trans. Microwave Theory Tech.*, Vol. MTT-35, No. 3, March 1987.
- [5] Y. C. Shih and T. Itoh, "Analysis of Conductor-Backed Coplanar Waveguide," *Electronics Letters*, Vol. 18, No. 12, June 1982.
- [6] E. O. Hammerstad and F. Bekkadal, *A Microstrip Handbook*, ELAB Report, STF 44 A74169, N7034, University of Trondheim, Norway, 1975.

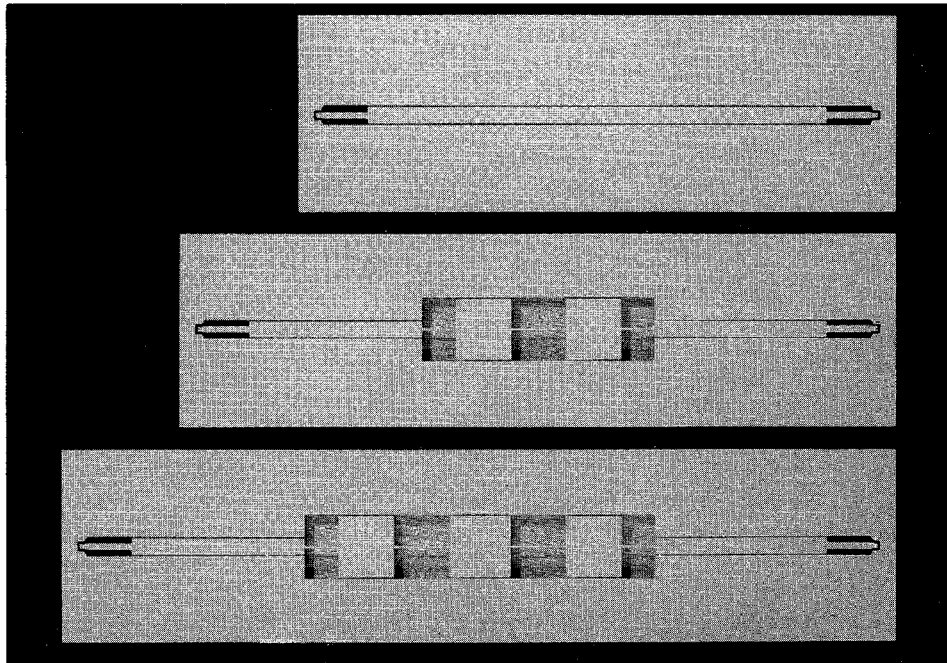


Figure 1: Photograph of a 5- and a 7-section microshield stepped-impedance low pass filter. The upper metallization is  $340 \mu\text{m}$  from the lower ground plane, producing the shadows which are seen around the center conductor and upper ground plane edges. The thin center conductor sections are  $40 \mu\text{m}$  wide and the width of all ground planes is  $0.42 \text{ cm}$ . The grounded coplanar waveguide-to-microshield transitions occur where the line narrows on either end of the circuits.

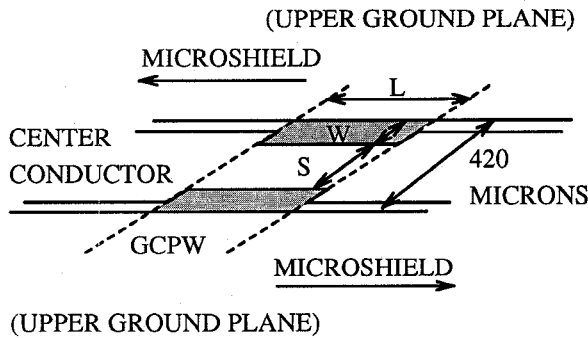


Figure 2: Illustration of the microshield to grounded cpw (coplanar waveguide) transition. The center conductor width,  $S$ , the slot width,  $W$ , and the length of the gcpw,  $L$ , are all indicated.  $L$  is  $\frac{\lambda_0}{2}$  at  $40 \text{ GHz}$ . The slots in the gcpw are shaded to indicate that the substrate dielectric changes from air in the microshield to silicon in the gcpw section.

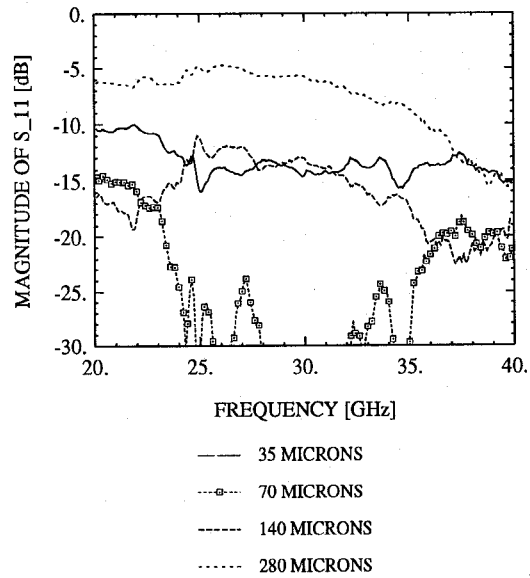


Figure 3: Measured  $S_{11}$  response of four different microshield to grounded cpw transitions. The microshield center conductor width is  $350 \mu\text{m}$ . Each plot corresponds to a different center conductor width for the gcpw. In all cases,  $2s+w$  is  $420 \mu\text{m}$  for both microshield and gcpw lines.

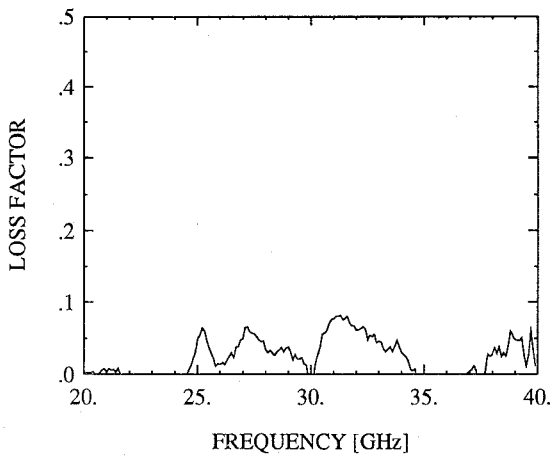


Figure 4: Measured loss factor,  $(1 - |S_{11}|^2 - |S_{21}|^2)$ , for the 70 micron microshield to grounded cpw transition.

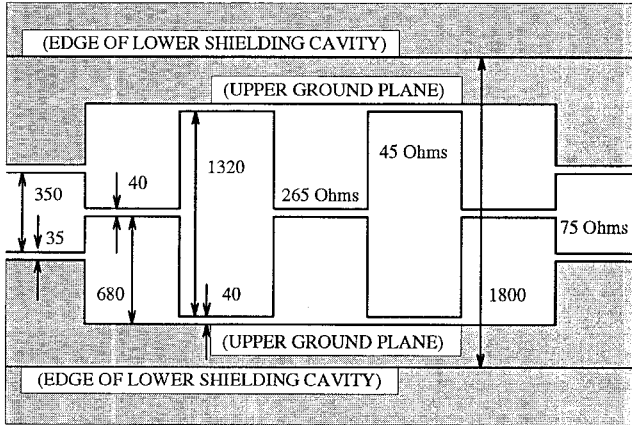


Figure 5: Diagram of the 5-section stepped-impedance low-pass filter (not to scale). Dimensions are given in  $\mu\text{m}$  and the different impedance sections are also indicated. The shaded regions are the upper ground planes, which have been marked to indicate the positions of the lower shielding cavity sidewalls.

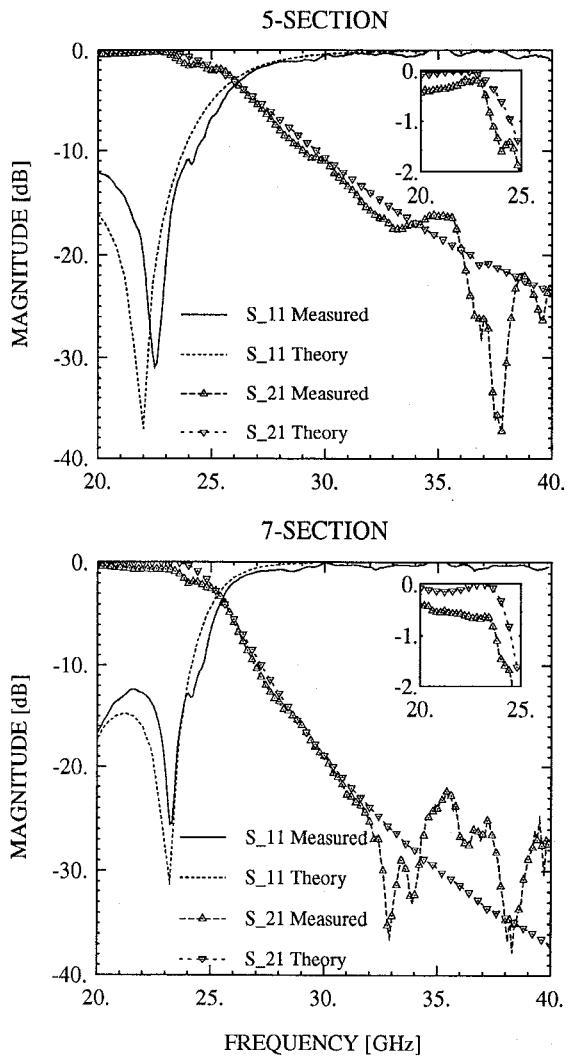


Figure 6: Measured and theoretical response of a 5- and a 7-section stepped-impedance microshield filter.

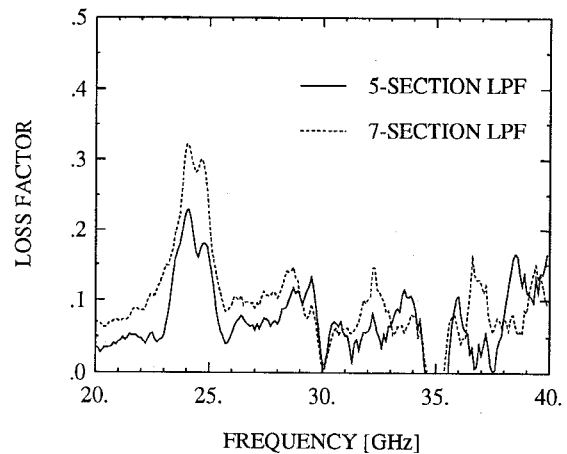


Figure 7: Measured loss factor,  $(1 - |S_{11}|^2 - |S_{21}|^2)$ , for the 5- and 7-section low pass filters.